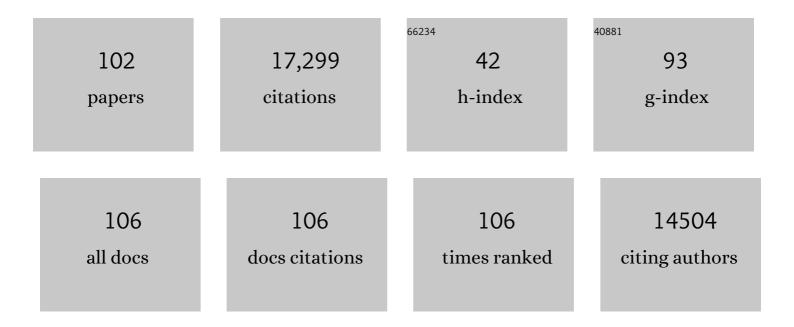
Jingyue Liu

List of Publications by Year in descending order

Source: https://exaly.com/author-pdf/3480909/publications.pdf Version: 2024-02-01



LINCYLIE LILL

#	Article	IF	CITATIONS
1	Single-atom catalysis of CO oxidation using Pt1/FeOx. Nature Chemistry, 2011, 3, 634-641.	6.6	5,149
2	Single-Atom Catalysts: A New Frontier in Heterogeneous Catalysis. Accounts of Chemical Research, 2013, 46, 1740-1748.	7.6	3,405
3	Catalysis by Supported Single Metal Atoms. ACS Catalysis, 2017, 7, 34-59.	5.5	1,047
4	FeOx-supported platinum single-atom and pseudo-single-atom catalysts for chemoselective hydrogenation of functionalized nitroarenes. Nature Communications, 2014, 5, 5634.	5.8	890
5	Platinum-based nanocages with subnanometer-thick walls and well-defined, controllable facets. Science, 2015, 349, 412-416.	6.0	854
6	Palladium–platinum core-shell icosahedra with substantially enhanced activity and durability towards oxygen reduction. Nature Communications, 2015, 6, 7594.	5.8	440
7	Highly Efficient Catalysis of Preferential Oxidation of CO in H ₂ -Rich Stream by Gold Single-Atom Catalysts. ACS Catalysis, 2015, 5, 6249-6254.	5.5	380
8	Structure of the catalytically active copper–ceria interfacial perimeter. Nature Catalysis, 2019, 2, 334-341.	16.1	368
9	Pd@Pt Core–Shell Concave Decahedra: A Class of Catalysts for the Oxygen Reduction Reaction with Enhanced Activity and Durability. Journal of the American Chemical Society, 2015, 137, 15036-15042.	6.6	296
10	Catalysis on singly dispersed bimetallic sites. Nature Communications, 2015, 6, 7938.	5.8	235
11	Pt-Based Icosahedral Nanocages: Using a Combination of {111} Facets, Twin Defects, and Ultrathin Walls to Greatly Enhance Their Activity toward Oxygen Reduction. Nano Letters, 2016, 16, 1467-1471.	4.5	228
12	Supported Single Pt ₁ /Au ₁ Atoms for Methanol Steam Reforming. ACS Catalysis, 2014, 4, 3886-3890.	5.5	204
13	Ultrastable Hydroxyapatite/Titaniumâ€Dioxideâ€Supported Gold Nanocatalyst with Strong Metal–Support Interaction for Carbon Monoxide Oxidation. Angewandte Chemie - International Edition, 2016, 55, 10606-10611.	7.2	192
14	Bifunctional Ag@Pd-Ag Nanocubes for Highly Sensitive Monitoring of Catalytic Reactions by Surface-Enhanced Raman Spectroscopy. Journal of the American Chemical Society, 2015, 137, 7039-7042.	6.6	184
15	Theoretical and Experimental Investigations on Single-Atom Catalysis: Ir ₁ /FeO _{<i>x</i>} for CO Oxidation. Journal of Physical Chemistry C, 2014, 118, 21945-21951.	1.5	145
16	Pocketlike Active Site of Rh ₁ /MoS ₂ Single-Atom Catalyst for Selective Crotonaldehyde Hydrogenation. Journal of the American Chemical Society, 2019, 141, 19289-19295.	6.6	141
17	Identifying Size Effects of Pt as Single Atoms and Nanoparticles Supported on FeO _{<i>x</i>} for the Water-Gas Shift Reaction. ACS Catalysis, 2018, 8, 859-868.	5.5	140
18	Radially Aligned Porous Carbon Nanotube Arrays on Carbon Fibers: A Hierarchical 3D Carbon Nanostructure for Highâ€Performance Capacitive Energy Storage. Advanced Functional Materials, 2016, 26, 3012-3020.	7.8	132

JINGYUE LIU

#	Article	IF	CITATIONS
19	Catalytically Active Rh Subâ€Nanoclusters on TiO ₂ for CO Oxidation at Cryogenic Temperatures. Angewandte Chemie - International Edition, 2016, 55, 2820-2824.	7.2	127
20	Ultrathin, Polycrystalline, Two-Dimensional Co ₃ O ₄ for Low-Temperature CO Oxidation. ACS Catalysis, 2019, 9, 2558-2567.	5.5	116
21	High-Indexed Pt ₃ Ni Alloy Tetrahexahedral Nanoframes Evolved through Preferential CO Etching. Nano Letters, 2017, 17, 2204-2210.	4.5	113
22	Identification of Active Area as Active Center for CO Oxidation over Single Au Atom Catalyst. ACS Catalysis, 2020, 10, 6094-6101.	5.5	106
23	Dual Metal Active Sites in an Ir ₁ /FeO _{<i>x</i>} Singleâ€Atom Catalyst: A Redox Mechanism for the Waterâ€Gas Shift Reaction. Angewandte Chemie - International Edition, 2020, 59, 12868-12875.	7.2	102
24	Ferric Oxide-Supported Pt Subnano Clusters for Preferential Oxidation of CO in H ₂ -Rich Gas at Room Temperature. ACS Catalysis, 2014, 4, 2113-2117.	5.5	96
25	Remarkable active-site dependent H2O promoting effect in CO oxidation. Nature Communications, 2019, 10, 3824.	5.8	96
26	CO Oxidation on Metal Oxide Supported Single Pt atoms: The Role of the Support. Industrial & Engineering Chemistry Research, 2017, 56, 6916-6925.	1.8	94
27	Highly active Au1/Co3O4 single-atom catalyst for CO oxidation at room temperature. Chinese Journal of Catalysis, 2015, 36, 1505-1511.	6.9	93
28	Remarkable effect of alkalis on the chemoselective hydrogenation of functionalized nitroarenes over high-loading Pt/FeO _x catalysts. Chemical Science, 2017, 8, 5126-5131.	3.7	90
29	Activating low-temperature diesel oxidation by single-atom Pt on TiO2 nanowire array. Nature Communications, 2020, 11, 1062.	5.8	90
30	Facile Synthesis of Ag Nanorods with No Plasmon Resonance Peak in the Visible Region by Using Pd Decahedra of 16 nm in Size as Seeds. ACS Nano, 2015, 9, 10523-10532.	7.3	88
31	Single atom gold catalysts for low-temperature CO oxidation. Chinese Journal of Catalysis, 2016, 37, 1580-1586.	6.9	85
32	Kinetically Controlled Synthesis of Pd–Cu Janus Nanocrystals with Enriched Surface Structures and Enhanced Catalytic Activities toward CO ₂ Reduction. Journal of the American Chemical Society, 2021, 143, 149-162.	6.6	77
33	Photochemical Deposition of Highly Dispersed Pt Nanoparticles on Porous CeO ₂ Nanofibers for the Waterâ€Gas Shift Reaction. Advanced Functional Materials, 2015, 25, 4153-4162.	7.8	75
34	One-Pot Synthesis of Penta-twinned Palladium Nanowires and Their Enhanced Electrocatalytic Properties. ACS Applied Materials & Interfaces, 2017, 9, 31203-31212.	4.0	70
35	The shape effect of TiO ₂ in VO _x /TiO ₂ catalysts for selective reduction of NO by NH ₃ . Journal of Materials Chemistry A, 2015, 3, 14409-14415.	5.2	65
36	Ultrastable 3V-PPh3 polymers supported single Rh sites for fixed-bed hydroformylation of olefins. Journal of Molecular Catalysis A, 2015, 404-405, 211-217.	4.8	65

Jingyue Liu

#	Article	IF	CITATIONS
37	Gold-Based Cubic Nanoboxes with Well-Defined Openings at the Corners and Ultrathin Walls Less Than Two Nanometers Thick. ACS Nano, 2016, 10, 8019-8025.	7.3	65
38	Advanced Electron Microscopy Characterization of Nanostructured Heterogeneous Catalysts. Microscopy and Microanalysis, 2004, 10, 55-76.	0.2	63
39	Aberration-corrected scanning transmission electron microscopy in single-atom catalysis: Probing the catalytically active centers. Chinese Journal of Catalysis, 2017, 38, 1460-1472.	6.9	63
40	Identification of Active Sites on High-Performance Pt/Al ₂ O ₃ Catalyst for Cryogenic CO Oxidation. ACS Catalysis, 2020, 10, 8815-8824.	5.5	54
41	Geometrical Structure of the Gold–Iron(III) Oxide Interfacial Perimeter for CO Oxidation. Angewandte Chemie - International Edition, 2018, 57, 11289-11293.	7.2	53
42	Superior activity of Rh1/ZnO single-atom catalyst for CO oxidation. Chinese Journal of Catalysis, 2019, 40, 1847-1853.	6.9	47
43	Strong Coupling between ZnO Excitons and Localized Surface Plasmons of Silver Nanoparticles Studied by STEM-EELS. Nano Letters, 2015, 15, 5926-5931.	4.5	42
44	More active Ir subnanometer clusters than singleâ€atoms for catalytic oxidation of CO at low temperature. AICHE Journal, 2017, 63, 4003-4012.	1.8	41
45	Facile Fabrication of SnO ₂ Nanorod Arrays Films as Electron Transporting Layer for Perovskite Solar Cells. Solar Rrl, 2018, 2, 1800133.	3.1	41
46	Toward the Design of a Hierarchical Perovskite Support: Ultra-Sintering-Resistant Gold Nanocatalysts for CO Oxidation. ACS Catalysis, 2017, 7, 3388-3393.	5.5	40
47	A highly active Pt–Fe/Ĵ³-Al ₂ O ₃ catalyst for preferential oxidation of CO in excess of H ₂ with a wide operation temperature window. Chemical Communications, 2017, 53, 9020-9023.	2.2	40
48	Highly crystalline Nb-doped TiO ₂ nanospindles as superior electron transporting materials for high-performance planar structured perovskite solar cells. RSC Advances, 2018, 8, 20982-20989.	1.7	40
49	Syntheses, Plasmonic Properties, and Catalytic Applications of Ag–Rh Core-Frame Nanocubes and Rh Nanoboxes with Highly Porous Walls. Chemistry of Materials, 2018, 30, 2151-2159.	3.2	39
50	Coating Pt–Ni Octahedra with Ultrathin Pt Shells to Enhance the Durability without Compromising the Activity toward Oxygen Reduction. ChemSusChem, 2016, 9, 2209-2215.	3.6	35
51	Hetero-epitaxially anchoring Au nanoparticles onto ZnO nanowires for CO oxidation. Chemical Communications, 2015, 51, 15332-15335.	2.2	34
52	Observing the Overgrowth of a Second Metal on Silver Cubic Seeds in Solution by Surface-Enhanced Raman Scattering. ACS Nano, 2017, 11, 5080-5086.	7.3	34
53	Stable and solubilized active Au atom clusters for selective epoxidation of cis-cyclooctene with molecular oxygen. Nature Communications, 2017, 8, 14881.	5.8	34
54	Single-atom catalysis for a sustainable and greener future. Current Opinion in Green and Sustainable Chemistry, 2020, 22, 54-64.	3.2	33

JINGYUE LIU

#	Article	IF	CITATIONS
55	Catalytically Active Rh Subâ€Nanoclusters on TiO ₂ for CO Oxidation at Cryogenic Temperatures. Angewandte Chemie, 2016, 128, 2870-2874.	1.6	31
56	Fiveâ€Fold Twinned Pd Nanorods and Their Use as Templates for the Synthesis of Bimetallic or Hollow Nanostructures. ChemNanoMat, 2015, 1, 246-252.	1.5	30
57	Ultrastable Hydroxyapatite/Titaniumâ€Dioxideâ€Supported Gold Nanocatalyst with Strong Metal–Support Interaction for Carbon Monoxide Oxidation. Angewandte Chemie, 2016, 128, 10764-10769.	1.6	29
58	A Rationally Designed Route to the One-Pot Synthesis of Right Bipyramidal Nanocrystals of Copper. Chemistry of Materials, 2018, 30, 6469-6477.	3.2	28
59	Hollow carbon anchored highly dispersed Pd species for selective hydrogenation of 3-nitrostyrene: metal-carbon interaction. Chemical Communications, 2018, 54, 13248-13251.	2.2	25
60	Atomic scale observation of oxygen delivery during silver–oxygen nanoparticle catalysed oxidation of carbon nanotubes. Nature Communications, 2016, 7, 12251.	5.8	24
61	Highly Active Small Palladium Clusters Supported on Ferric Hydroxide for Carbon Monoxide‶olerant Hydrogen Oxidation. ChemCatChem, 2014, 6, 547-554.	1.8	23
62	A Dual Catalyst with SERS Activity for Probing Stepwise Reduction and Oxidation Reactions. ChemNanoMat, 2016, 2, 786-790.	1.5	22
63	Facet-Selective Epitaxial Growth of δ-Bi ₂ O ₃ on ZnO Nanowires. Chemistry of Materials, 2016, 28, 8141-8148.	3.2	22
64	Nanocarbon-Edge-Anchored High-Density Pt Atoms for 3-nitrostyrene Hydrogenation: Strong Metal-Carbon Interaction. IScience, 2019, 13, 190-198.	1.9	22
65	lr ₁ Zn <i>_n</i> Bimetallic Site for Efficient Production of Hydrogen from Methanol. ACS Sustainable Chemistry and Engineering, 2019, 7, 18793-18800.	3.2	19
66	Synthesis of Ag/PANI@MnO ₂ core–shell nanowires and their capacitance behavior. RSC Advances, 2016, 6, 17415-17422.	1.7	18
67	Advances and Applications of Atomic-Resolution Scanning Transmission Electron Microscopy. Microscopy and Microanalysis, 2021, 27, 943-995.	0.2	14
68	Probing the catalytic behavior of ZnO nanowire supported Pd 1 single-atom catalyst for selected reactions. Chinese Journal of Catalysis, 2017, 38, 1549-1557.	6.9	13
69	Catalysis by Supported Single Metal Atoms. Microscopy and Microanalysis, 2016, 22, 860-861.	0.2	12
70	Geometrical Structure of the Gold–Iron(III) Oxide Interfacial Perimeter for CO Oxidation. Angewandte Chemie, 2018, 130, 11459-11463.	1.6	12
71	Structure and morphology of polar and semi-polar pyramidal surfaces coating wurtzite ZnO micro-wires. Journal of Materials Science, 2013, 48, 3857-3862.	1.7	10
72	Atomic-Scale Structure and Catalysis on Positively Charged Bimetallic Sites for Generation of H ₂ . Nano Letters, 2020, 20, 6255-6262.	4.5	10

Jingyue Liu

#	Article	IF	CITATIONS
73	Geometric effect of Au nanoclusters on room temperature CO oxidation. Chemical Communications, 2020, 56, 876-879.	2.2	8
74	Facet Selective Growth of Iridium Chains/Wires of Single-Atom Width on the {1010} Surfaces of ZnO Nanowires. Microscopy and Microanalysis, 2017, 23, 484-485.	0.2	6
75	Surface Channeling in Aberration-Corrected Scanning Transmission Electron Microscopy of Nanostructures. Microscopy and Microanalysis, 2010, 16, 425-433.	0.2	5
76	Pt ₁ –O ₄ as active sites boosting CO oxidation <i>via</i> a non-classical Mars–van Krevelen mechanism. Catalysis Science and Technology, 2021, 11, 3578-3588.	2.1	5
77	Synthesis of Anchored Bimetallic Catalysts via Epitaxy. Catalysts, 2016, 6, 88.	1.6	3
78	Imaging at the Single-Atom Level in Closed-Cell In Situ Gas Reactions. Microscopy and Microanalysis, 2016, 22, 876-877.	0.2	3
79	Manipulation of Pt-Ni Tetrahexahedral Nanoframes Using a Gaseous Etching Method. MRS Advances, 2018, 3, 943-948.	0.5	3
80	Facile Synthesis of Pdâ^'Cu Bimetallic Twin Nanocubes and a Mechanistic Understanding of the Shape Evolution. ChemNanoMat, 2020, 6, 386-391.	1.5	3
81	Aberration-corrected STEM Study of Atomically Dispersed Pti/FeOx Catalyst with High Loading of Pt. Microscopy and Microanalysis, 2015, 21, 1733-1734.	0.2	2
82	Template Synthesis of Hollow Carbon Nanofibers. Microscopy and Microanalysis, 2015, 21, 989-990.	0.2	2
83	Nanotube Arrays: Radially Aligned Porous Carbon Nanotube Arrays on Carbon Fibers: A Hierarchical 3D Carbon Nanostructure for High-Performance Capacitive Energy Storage (Adv. Funct. Mater.) Tj ETQq1 1 0.78	843 7. % rgB ⁻	Г /Qverlock 1
84	Two-dimensional Polycrystalline Co ₃ O ₄ Supported High-Number-Density Metal Single Atoms and Clusters. Microscopy and Microanalysis, 2019, 25, 2210-2211.	0.2	2
85	Synthesis of Na@nanoFAU Zeolite Catalyst and Catalysis for Production of Formic Acid with Na@nanoFAU. Catalysis Letters, 2019, 149, 1965-1974.	1.4	2
86	In Situ Investigation of the Carbothermal Reduction of ZnO Nanowires. Microscopy and Microanalysis, 2014, 20, 1554-1555.	0.2	1
87	Strong Coupling between ZnO Exciton and Localized Surface Plasmon in Ag Nanoparticles Studied by STEM-EELS. Microscopy and Microanalysis, 2015, 21, 1685-1686.	0.2	1
88	ZnO Nanowire Supported Metal Single Atoms for CO oxidation. Microscopy and Microanalysis, 2016, 22, 872-873.	0.2	1
89	The Stability of High Metal-Loading Pt1/Fe2O3 Single-Atom Catalyst Under Different Gas Environment. Microscopy and Microanalysis, 2017, 23, 1898-1899.	0.2	1
90	Development of Two-Dimensional Polycrystalline C03O4 Hierarchical Structures and Pt1/2D-Co3O4 Single-atom Catalysts. Microscopy and Microanalysis, 2017, 23, 1868-1869.	0.2	1

JINGYUE LIU

#	Article	IF	CITATIONS
91	Anchoring Pt Single Atoms on CeOx Nanoclusters for CO Oxidation. Microscopy and Microanalysis, 2018, 24, 1660-1661.	0.2	1
92	Challenges in Determining Structure of Supported Subnano Metal Clusters. Microscopy and Microanalysis, 2019, 25, 1640-1641.	0.2	1
93	The Versatile Imaging Capabilities of Aberration-Corrected STEM. Microscopy and Microanalysis, 2014, 20, 88-89.	0.2	0
94	Aberration-corrected STEM of Four-atom Rhenium Nanowires Confined within Carbon Nanotubes. Microscopy and Microanalysis, 2015, 21, 2255-2256.	0.2	0
95	In Situ Observation of Ag Nanoparticle Catalyzed Oxidation of Carbon Nanotubes in an Aberration-corrected Environmental TEM. Microscopy and Microanalysis, 2015, 21, 423-424.	0.2	0
96	Rücktitelbild: Catalytically Active Rh Subâ€Nanoclusters on TiO ₂ for CO Oxidation at Cryogenic Temperatures (Angew. Chem. 8/2016). Angewandte Chemie, 2016, 128, 2998-2998.	1.6	0
97	STEM-EELS Evaluation of the Dependence of Localized Surface Plasmon Linewidth on the Size of Au Nanoparticles. Microscopy and Microanalysis, 2017, 23, 1554-1555.	0.2	0
98	Pt1/CeO2-ZnO Nanowire Single-Atom Catalysts for Water-Gas Shift Reaction. Microscopy and Microanalysis, 2017, 23, 1856-1857.	0.2	0
99	Two-Dimensional Polycrystalline ZnO Hierarchical Structures as Single-atom Catalyst Supports. Microscopy and Microanalysis, 2018, 24, 1604-1605.	0.2	0
100	Site Selective Growth of Noble Metal Atoms on Two-dimensional MoS2 Nanosheets. Microscopy and Microanalysis, 2018, 24, 1562-1563.	0.2	0
101	Synthesis of Ultrathin-Wall Mesoporous Cu2O Nanotubes for Low-Temperature Carbon Monoxide Oxidation. Microscopy and Microanalysis, 2019, 25, 2244-2245.	0.2	0
102	Probing the Active Sites of ZnO Nanowire Supported Ir Species for CO Oxidation. Microscopy and Microanalysis, 2019, 25, 2204-2205.	0.2	0